Jour. Geol. Soc. India (2022) 98:1653-1660
https://doi.org/10.1007/s12594-022-2233-5

ORIGINAL ARTICLE

Geochemical Trends and Rare Earth Elements' Behaviour in the Recently Exposed Weathering Profiles of the Deccan Basalts from Central India

Anuradha Patel, Rachna Raj and Jayant K. Tripathi*
School of Environmental Sciences, Jawaharlal Nehru University, New Delhi - 110 067, India
***E-mail:** jktrip@yahoo.com*

Received: 31 May 2022 / Revised form Accepted: 20 September 2022

ABSTRACT

The Deccan basalts have been undergoing intense weathering in the tropical conditions since the passage of India through the equator. This study is on the basalts' weathering from central India's present-day semiarid climate. Two weathering profiles from the districts of Indore and Dhar, Madhya Pradesh, have been studied using mineralogy and geochemistry. The profiles show incipient weathering with low to medium Chemical Index of Alteration (CIA) and Mafic Index of Alteration-oxidising ($MIA_{(O)}$) values. The presence of smectite in weathered zones, mineralogically attests to incipient weathering. The pyroxene and plagioclase-rich zones have produced smectite clays in the basalts. The rare earth elements (REE) and, to a greater extent, the heavy (H) REE show mobility during incipient weathering, which appears to be due to differential retention of REE in the clay minerals. The smectites seem to retain light (L) REE more significantly than HREE. The ancient terrain showing currently incipient weathering indicates recent exposure of the profiles by the erosion under neotectonic activity. In this fashion, the frequent exposures of new weathering surfaces on the basalts may have played a significant role in the uninterrupted consumption of CO_2 by silicate weathering since around 50 Ma.

INTRODUCTION

Basalt weathering is crucial to the Earth because of its capability to sequester atmospheric CO_2 most effectively among other prevalent rock types (Kent and Muttoni, 2013; Babechuk et al., 2014). Thermodynamically, unstable minerals of basalts undergo fast weathering on the Earth's surface, contributing to global geochemical cycles (Babechuk et al., 2014 and references therein). The continental basalts in the humid equatorials play a vital role in soaking CO_2 from the atmosphere via silicate weathering (Conwell et al., 2022). The Deccan Volcanic Province (DVP) transit through the humid equatorial since around 50 Ma accompanied by the Ethiopian Traps, may have significantly consumed CO_2 by silicate weathering (Kent and Muttoni, 2013 and references therein). Whenever mafic/ultramafic rocks of arc-continent collisions were exhumed and weathered in the tropics, the Earth entered the cooling phase during the Phanerozoic (Conwell et al., 2022). Chemical weathering processes decompose primary minerals and remove alkali and alkaline metals to produce sediments that are mineralogically and geochemically different from the parent rocks (Nesbitt and Markovics, 1997). The dissolved components of weathering products, e.g., Ca^{2+} and HCO_3^-, are delivered to fluvial and marine systems. These ions are biologically consumed and deposited as thick carbonate rocks on the ocean floors, which locks CO_2 and regulates long-term climate (Rau et al., 2007). However, relatively immobile elements get added to the continents through weathering, erosion, physical transport, diagenesis and metamorphism, contributing to the crustal evolution (Taylor and McLennan, 1985). REE belong to that category and explains the crustal evolution, i.e., from the less fractionated REE pattern (without Eu depletion) of the mafic Archean upper crust to the fractionated REE pattern (with Eu depletion) of the felsic post Archean upper crust (Taylor and McLennan, 1985). Rocks get progressively enriched in LREE with igneous differentiation processes; therefore, various igneous rocks and their descendant sediments can be identified by the REE patterns as, generally, REE do not mobilize during weathering (Taylor and McLennan et al., 1985). However, many studies report their mobilization during intense weathering (Tripathi and Rajamani, 2007 and references therein).

The DVP, covering almost 15% of the geographical area of India, controls the sediment and water composition of the rivers traversing through the peninsula (Tripathi et al., 2013 and references therein). However, only limited studies have undertaken on the in situ weathering on the Deccan basalts, e.g., Babechuk et al. (2014) and Liu et al. (2019). Basalts exposed to the surface have a high potential for weathering and CO_2 sequestration, because they contain thermodynamically highly unstable minerals (Eggleton et al, 1987). However, extensive weathering forms lateritic cover, which slows down further weathering (Godderis et al., 2008). The geochemical trends are presented in two exposed, non-lateritic basalt weathering profiles and their control on REE behaviour to explain its implications for CO_2 sequestration and climate.

STUDY AREA

The DVP is an extensive continental flood basalt (Fig. 1a) emplaced during the Cretaceous–Palaeogene boundary (Babechuk et al., 2014). The tholeiitic basalts with subordinate picrites, picritic, and alkaline basalts make up the DVP (Vaidyanadhan and Ramakrishnan, 2008). This study has been carried out on the two weathering profiles developed on the basalts in the semiarid climate (Reddy, 1983) of the Indore and Dhar districts (Fig. 1b). The soils of

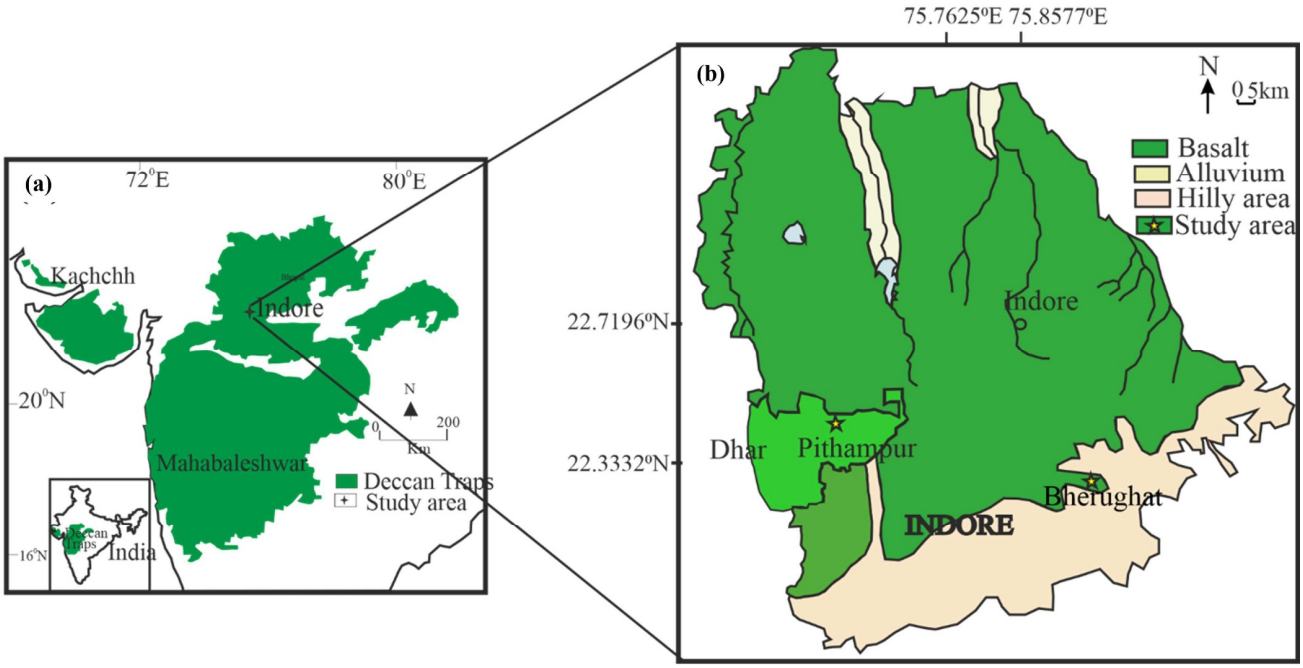

Fig. 1. Geological map of the Deccan Volcanic Province (modified after Vaidyanadhan and Ramakrishanan 2008) (a), Geological map of the study area around Indore and Dhar (CGWB, 2013a and b) (b).

the study area are black soils defined as vertisols (Parmar and Sharma, 2020).

SAMPLING AND ANALYTICAL METHODS

Two weathered profiles developed on the basalts have been studied. The Pithampur profile (PSJ) is located in the Dhar district (N 22°35'15"; E 75°40'02"), and the Bherughat profile (BHG-B) is located in the Indore district (N 22°27'53"; E 75°56'10"). The thickness of the profile of Bherughat is 2.5 m, and Pithampur is 7.5 m. Both the weathering profiles are continuous from the parent basalt to the topsoil. They show distinct layers of parent rocks, saproliths with lithic nature and joints, and saprolites with faint exfoliation fractures (Fig. 2a and 2b). The top 15 to 20 cm is loose soil with rootlets and without agricultural practices. Some climber plants growing from the exposed saprolite surface have also been observed (Fig. 2a).

The parent basalt, saprolith, and saprolite samples from both the profiles were collected in pre-cleaned zipped pouches. The samples were air-dried and stored before processing for mineralogical and geochemical analysis. The saprolite samples were sieved (<2 mm) before pH measurement, following Jiang et al. (2018) using LMPH-10 pH meter. Thin sections of the rocks were studied under a polarizing microscope (NIKON LV100POL) at Delhi University, New Delhi. The mineralogy of saproliths and saprolites was analyzed using Philips X'pert pro XRD at IUAC, New Delhi. The clay minerals were identified using FTIR (Varian 7000) at AIRF, JNU, New Delhi.

Pulverized and homogenized samples of 200 mesh size (<75 µm), for better representation of the whole sample, (see Raj et al. 2021 for sample preparation) were used for bulk XRD mineralogy and geochemical analyses. For the clay minerals analysis, XRD was done for air dried and Ca saturated ethylene glycol treated, and FTIR was done for >63 µm fraction of saprolites. The major and trace elements analysis by WD-XRF (PANalytical, Axios) and REE analysis by ICP-MS (iCAPQ, Thermo Fisher Scientific) were done at IUAC, New Delhi. See Raj et al. (2021) for pellet preparation for XRF, and Khanna et al. (2009) for acid digestion for ICP-MS analysis. The loss on ignition analysis was determined after keeping the sample at 105 °C for 12 hours for water removal, 550 °C for 4 hours for organic matter removal, and 950°C for 2 hours for inorganic carbon removal, following Heiri et al. (2001).

International rock standards of USGS (GSP-2, BHVO-2, AVG-2), GSJ (JA-2, JA-3, JB-1b), and MBH from WIHG, India, have been used for calibration of the instruments and as reference samples for the instrument stability during the analysis. The analytical precision for major oxides was better than 5% and better than 10% for trace elements. The precision for REE analysis was better than 5% for the ICP-MS analysis.

The Chemical index of alteration (CIA) has been calculated to understand the extent of weathering, and the A-CN-K and A-CNK-FM diagrams have been plotted to illustrate weathering trends (Nesbitt and Young, 1989). The common primary igneous silicate minerals, secondary clay minerals and common igneous rocks can be well represented in these plots (Fedo et al., 1995). Mg and Fe also get mobilized during weathering of mafic minerals. Hence, for the oxidizing weathering conditions, Babechuk et al., (2014) have proposed mafic index of alteration ($MIA_{(O)}$). The $MIA_{(O)}$ has been calculated for the exposed profiles, and the A-CNKM-F and AF-CNK-M diagrams have been plotted to understand weathering trends of mafic minerals (Babechuk et al., 2014). A, C, N, K, F, and M are Al_2O_3, CaO, Na_2O, K_2O, Fe_2O_3, and MgO in molar proportions, respectively. In the formula of CIA and values of C in the diagrams, the CaO present in the silicate phase only has been considered. The CaO in silicates has been calculated by subtracting CaO as carbonates and phosphates from the total CaO (see Fedo et al. 1995 for more details). The carbonate and phosphate values were obtained from the LOI at 950 °C and chemical analysis, respectively.

To understand mobilization/addition of elements, the % change is calculated assuming no volume change between weathering product and parent-rock (Babechuk et al., 2014). Al has been considered as conservative element (Srivastava et al., 2018).

RESULTS

Soil pH controls elemental mobility. The upper saprolites show lower pH (due to rainwater, soil CO_2 dissolution, and organic acids) than the lower saprolites, suggesting neutralization by weathering in

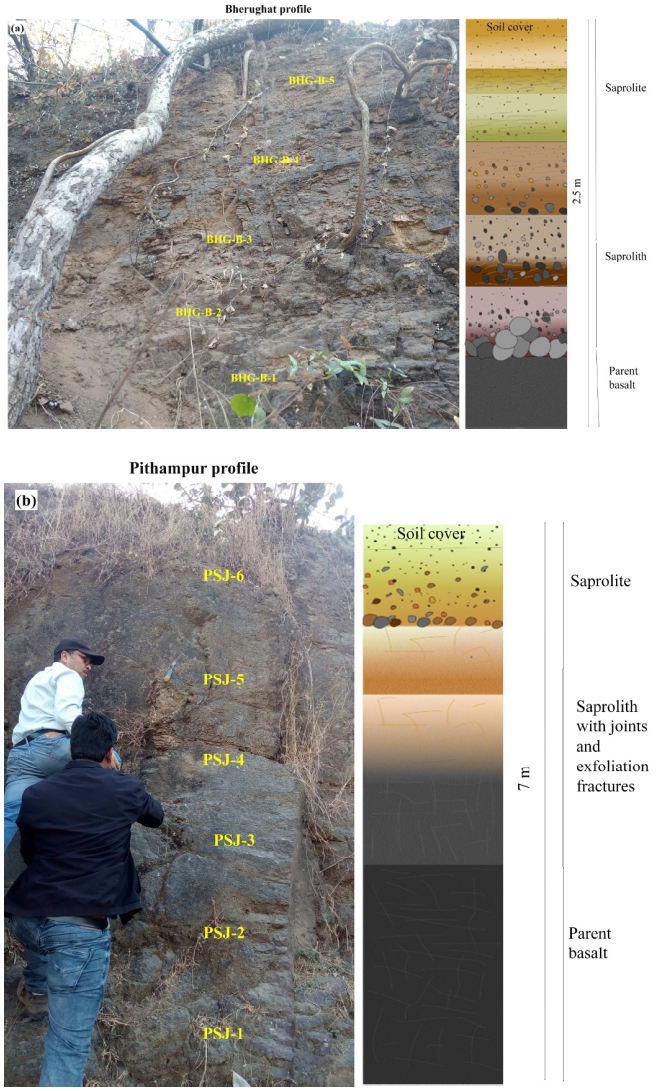

Fig. 2. Weathering profiles developed on the Deccan basalts showing various stages of weathering as seen exposed at Bherughat, Indore (a), and Pithampur, Dhar (b).

the lower saprolites (see Table 1). Elements are more mobile in acidic than in alkaline conditions (Ling et al., 2016). The unweathered parent rocks show the lowest LOI (BHG-B-10= 0.26% and PSJ-1= 2.65%). Whereas, with an increasing trend the most weathered samples show the highest LOI values (PSJ-1= 8.16% and BHG-B-1= 5.44%).

The bulk XRD mineralogy of the basalts shows mainly pyroxene and plagioclase (Griffin, 1971). Petrographic analysis of the basalts also suggests identical mineralogy (Fig. 3a, 3d). There is a strong peak at 15Å in the XRD of the bulk sample, which shifts from 15Å to 17Å after Ca saturated ethylene glycol treatment, suggesting the presence of smectite in the samples (Griffin, 1971) (Fig. 3b, 3e). The FTIR spectra' wave numbers (3620, 3400, 1650, 1040, and 915 cm^{-1}) confirm smectite's presence in the weathered samples (Kumpulainen and Kiviranta, 2010) (Fig. 3c, 3f).

The major elements (in oxide weight-percent) and trace elements (in ppm), including REE, data are given in Table 1. The parent-rocks of Bherughat and Pithampur plot in the field of basalts in the alkali-silica diagram (Klein and Philkpotts, 2017) (Fig. 4). The weathering trends of both the profiles are shown in the A-CN-K and A-CNK-FM diagrams (Fig. 5a and 5b). In the A-CN-K diagram, the parent-rocks and saproliths plot near the A-CN line, and saprolites away from it, along a weathering trend shown as an arrow (Nesbitt and Young, 1989), suggesting loss of Ca and Na and relative enrichment of Al during weathering. The CIA values (Table 1) of the parent-rocks and saproliths are close, indicating saproliths are physically altered products of the parent-rocks, exhibited by faint exfoliation fractures or friable when softly hammered. In the A-CNK-FM diagram, parent-rocks and saproliths plot nearby and saprolites away, showing A and FM enrichments. In the A-CNKM-F diagram (Fig. 5c), saprolites show loss of Ca, Na, K, and Mg and enrichment of Al and Fe. The $MIA_{(O)}$ values (Table-1) also suggest enrichment of Al. In the AF-CNK-M diagrams (Fig. 5d), samples plot along the arrow representing the loss of Ca, Na, and K. However, the uppermost saprolite (BHG-B-5) of Bherughat shows the higher loss in the M and enrichment in the AF component.

The chondrite normalized (after Masuda et al., 1973) parent-rocks' REE patterns are similar to other Deccan basalts (Kaotekwar et al., 2014). The REE patterns show LREE enrichment with fractionated HREE patterns, with minor negative Eu anomaly (Fig. 6a, 6b). The saprolite samples show HREE depletion after weathering.

DISCUSSION

Basalts are highly weatherable as they are composed of unstable minerals, such as olivine, pyroxene, and plagioclase (Eggleton et al., 1987). When the mobile elements are released during weathering, the primary minerals transform into clays and oxyhydroxide phases. Basalt weathering initially produces smectite and then kaolinite (Babechuk et al., 2014). Extensive weathering results in oxyhydroxides of Al, Fe, and Mn. The process and stages of weathering can be tracked using geochemistry and mineralogy of the parent rocks and weathering products. Therefore, here an attempt is to understand the extent and trend of weathering, geochemical changes vis-a-vis mineralogical transformations, and REE dynamics during weathering of the basalts.

Extent of Weathering

Both weathering indexes used in the study have a scale of 0-100, where 100 is designated for most weathered samples. The CIA values for the Pithampur (41.1 to 57.5) and Bherughat (35.5. to 42.7) profiles suggest incipient weathering has been suffered by the saprolites. The CIA value essentially tracks the weathering of feldspars, the release of mobile Ca, Na, and K relative to the immobile Al, and its retention in the pedogenic clays (Fedo et al., 1995). Whereas, the $MIA_{(O)}$ values track mafic minerals' weathering (Babechuk et al., 2014 and references therein). The $MIA_{(O)}$ values for the Pithampur (48.1 to 61.9) and Bherughat (41.4 to 48.9) also suggest incipient weathering shown by saprolites. The presence of smectite and absence of kaolinite/gibbsite in the clays support mineralogically the same. It is surmised that these basalts show incipient weathering due to their recent exposure. The recent neotectonic activities (Peshwa and Kale, 1997; Roy, 2006) could have eroded the regolith cover. The positioning of the DVP in the humid equatorial belt since around 50 Ma, the continuous tectonic activity due to stress generated by the India-Asia collision (Roy, 2006), help unceasing exposure of the new weathering surfaces and play a significant role in the consumption of CO_2 by silicate weathering (Kent and Muttoni, 2013).

Weathering Trends

It is essential to understand the trend and status of weathering, which is possible through major and trace elements. The A-CN-K framework mainly elucidate feldspar weathering in the rock. However, the AF-CNK-M and A-CNKM-F plots explain mafic minerals' weathering. Therefore, these plots shed more light on weathering trends of the basaltic rocks.

In the A-CN-K diagram (Fig. 5a), the parent-rocks plot on or near the A-CN line, suggesting the rocks are basalts made up of plagioclase and mafic minerals (see results section). In Bherughat, BHG-B-1

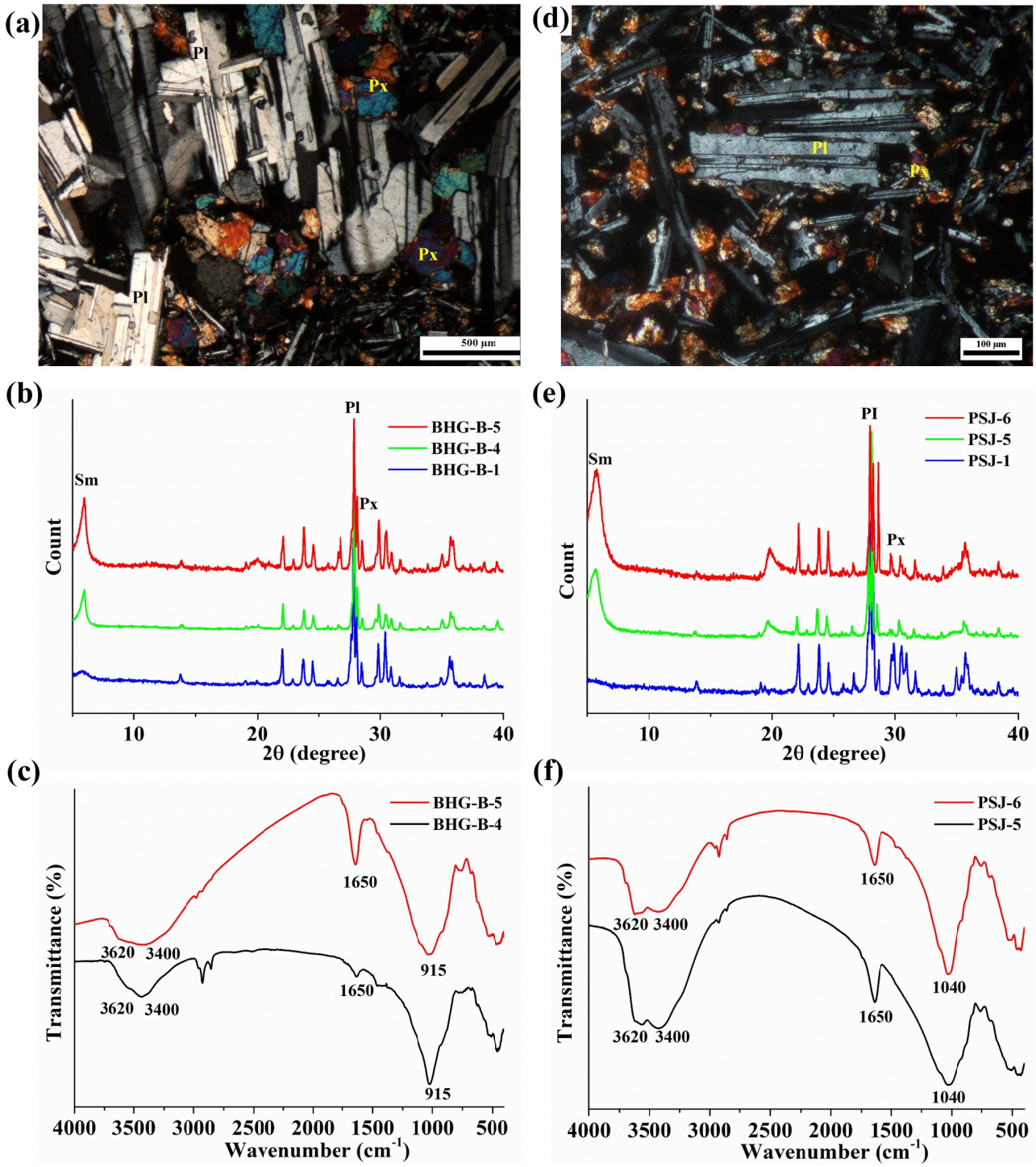

Fig. 3. Thin sections of parent-rocks of the Bherughat **(a)** and Pithampur **(d)** profiles under the microscope in the cross-polarized light show mainly plagioclase (Pl) and pyroxene (Px) minerals. XRD patterns of the respective saprolites show smectite peaks at the d value of ~15Å (bulk samples) **(b and e)**. The smectite peak in the clay fractions shifts from 15 Å to 17Å after Ca saturated ethylene glycol treatment (see inset of b and e). The FTIR spectrum for the saprolites shows smectite bands (c and f).

(parent-rock) and saproliths (BHG-B-2, and 3) plot nearby. Similarly, in Pithampur, PSJ-1 (parent-rock) and saproliths (PSJ-2, 3, and 4) plot nearby. Although parent-rocks and saproliths plot nearby, saproliths show physical weathering. The saprolite samples (BHG-B-4 and 5 and PSJ-5 and 6) plot beyond the respective parent-rocks/saproliths. They follow the expected normal weathering trend parallel to the A-CN line. This trend suggests the loss of CN components and the formation of smectites at the expense of pyroxenes and plagioclases. In the A-CNK-FM diagram (Figure 5B), the saproliths (BHG-2, 3 and PSJ-2, 3, 4) plot near the parent-rocks. The saprolites of Pithampur show a very similar trend of slight enrichment of A but a greater extent of FM. However, in Bherughat, saprolite (BHG-B-4) shows enrichment of FM, and sample BHG-B-5 shows enrichment of the A component. It is unclear from the A-CNK-FM diagram which one, among Fe and Mg, influences the FM component trend in the diagram. Therefore, AF-CNK-M and A-CNKM-F plots will be discussed below to better understand how the mafic components behave.

In the A-CNKM-F diagram (Fig. 5c), samples from both profiles follow trends of depletion of CNKM and the gain in A. Parent rocks and their saproliths also plot nearby, indicating only physical

Table 1. Major oxides (weight %), trace elements (ppm), and rare earth elements (ppm) data for the Bherughat and Pithampur basalt weathering profiles. CIA, MIA Ce/Ce*, and Eu/Eu* values have been calculated using the geochemical data and as per the standard methods of calculations (Nesbitt and Young, 1989, Babechuk et al., 2014, Taylor and McLennan, 1985).

	BHG-B-1	BHG-B-2	BHG-B-3	BHG-B-4	BHG-B-5	PSJ-1	PSJ-2	PSJ-3	PSJ-4	PSJ-5	PSJ-6
SiO_2	47.8	46.9	46.0	47.3	46.2	49.6	49.7	49.7	49.7	50.0	49.9
TiO_2	2.23	2.05	2.07	2.52	2.16	2.26	1.65	2.02	2.08	2.72	3.00
Al_2O_3	12.2	12.7	12.6	12.5	13.1	13.9	13.9	14.2	14.3	14.1	15.3
Fe_2O_3	12.4	13.8	12.7	14.6	12.0	12.4	12.5	12.6	12.6	13.1	13.1
MnO	0.19	0.11	0.14	0.10	0.19	0.19	0.17	0.17	0.16	0.10	0.08
MgO	8.17	8.46	8.12	10.43	5.48	4.37	4.77	4.55	4.30	5.46	5.02
CaO	9.95	11.0	11.5	8.74	8.81	9.55	9.98	10.00	10.09	6.57	6.05
Na_2O	1.64	1.71	1.76	1.43	1.38	2.48	2.43	2.24	2.41	1.09	1.12
K_2O	0.42	0.33	0.30	0.31	0.36	0.66	0.50	0.43	0.49	0.38	0.32
P_2O_5	0.32	0.24	0.23	0.22	0.25	0.26	0.33	0.32	0.31	0.30	0.29
% LOI	2.65	3.79	3.40	4.45	5.44	1.13	1.79	2.01	2.43	7.19	8.16
total	97.9	101.1	98.8	102.6	95.3	96.9	97.8	98.2	98.9	101.0	102.4
CIA	38.1	36.7	35.5	41.6	42.7	41.4	41.1	41.9	41.5	53.7	57.5
MIA	42.4	42.8	41.4	43.0	48.9	48.8	48.1	50.1	49.5	59.0	61.9
Ba	113	110	116	135	143	193	201	169	174	151	157
Sr	252	260	260	281	219	224	270	250	251	227	211
Cr	129	147	147	164	136	52	34	45	45	96	95
V	338	349	344	351	363	366	286	346	343	271	283
Ni	86	90	89	95	97	56	42	47	46	56	42
Cu	231	178	165	201	199	153	146	166	163	226	183
Co	48	42	44	47	52	44	37	39	38	42	28
Zn	112	95	95	109	177	105	83	104	95	118	112
Rb	9	7	6	5	12	18	20	20	21	17	16
Zr	82	108	107	156	99	126	161	175	173	176	145
Sc	37	38	34	52	39	19	28	19	27	52	49
La	18.0	15.8	15.4	13.6	19.4	21.4	23.3	21.4	21.2	20.2	22.0
Ce	40.5	34.1	33.7	30.9	40.8	44.4	49.3	45.7	43.9	39.2	41.2
Nd	25.8	21.4	21.4	17.8	23.8	26.8	30.7	27.9	27.2	26.9	28.4
Sm	6.44	5.16	5.30	4.42	5.81	6.89	7.85	7.05	6.91	6.76	7.24
Eu	1.88	1.63	1.69	1.51	1.75	1.93	2.30	2.05	2.00	1.98	2.03
Gd	5.69	4.87	4.71	3.85	5.42	6.39	7.22	6.34	6.29	6.02	6.20
Dy	6.08	4.78	4.92	3.57	5.72	6.88	7.27	6.67	6.52	5.67	5.97
Er	3.02	2.45	2.55	1.72	2.93	3.61	3.75	3.49	3.46	2.78	2.93
Yb	2.80	2.10	2.20	1.45	2.67	3.39	3.57	3.14	3.18	2.62	2.55
Lu	0.35	0.30	0.31	0.20	0.36	0.47	0.47	0.42	0.42	0.34	0.33
Ce/Ce*	0.95	0.92	0.93	0.98	0.92	0.90	0.91	0.92	0.90	0.83	0.83
Eu/Eu*	0.96	1.0	1.04	1.13	0.96	0.90	0.94	0.94	0.94	0.96	0.93
pH	-	-	7.9	7.9	7.8	-	-	-	-	7.7	7.4

weathering. However, saprolites show chemical weathering. In the AF-CNK-M diagram (Fig. 5d), the parent rocks and saproliths also plot nearby. In Pithampur, saprolites show CNK loss. The saprolites

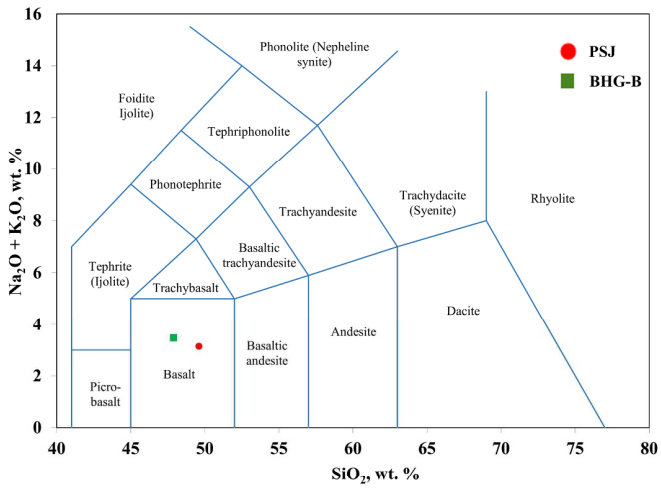

Fig. 4. In the total Alkali-Silica (TAS) diagram, the composition of parent rocks plot in the basalt field. Minerals present in the parent rocks also suggest basalt.

of Bherughat show different behaviour for AF and M during weathering. The BHG-B-4 shows an enrichment, but BHG-B-5 shows a depletion in M. Whereas BHG-B-4 shows a depletion for AF, BHG-B-5 shows a greater enrichment.

The geochemical mass balance plots (Fig. 7a, 7b) for Bherughat show Mg, Fe, and Ti enrichment in saprolite BHG-B-4. However, Mg gets depleted in BHG-B-5. In Pithampur (Fig. 7c, 7d) also, Mg shows enrichment in PSJ-5 and depletion in PSJ-6. Cr and Sc show enrichment in BHG-B-4 and PSJ-5 samples of profiles among the trace elements. Other elements do not show much variation, except for the depletion of alkalis and alkalines in saprolites.

From the weathering trends, it is clear that although the saproliths of profiles appear physically weathered, they have not undergone chemical weathering yet. The saprolites have experienced only a lesser extent of chemical weathering.

Mineral Transformation Geochemistry

The basalts from the study area contain pyroxene and plagioclase predominantly. The weathered materials trending parallel to the A-CN line in the A-CN-K plot suggest the advancement of weathering to produce smectite. The enrichment of Mg and Fe in the saprolites, as seen in AF-CNK-M and A-CNKM-F plots and geochemical mass balance plots (Fig. 7a, 7c), indicates the formation of smectite on weathering (Nesbitt and Young, 1989). The weathering indices and

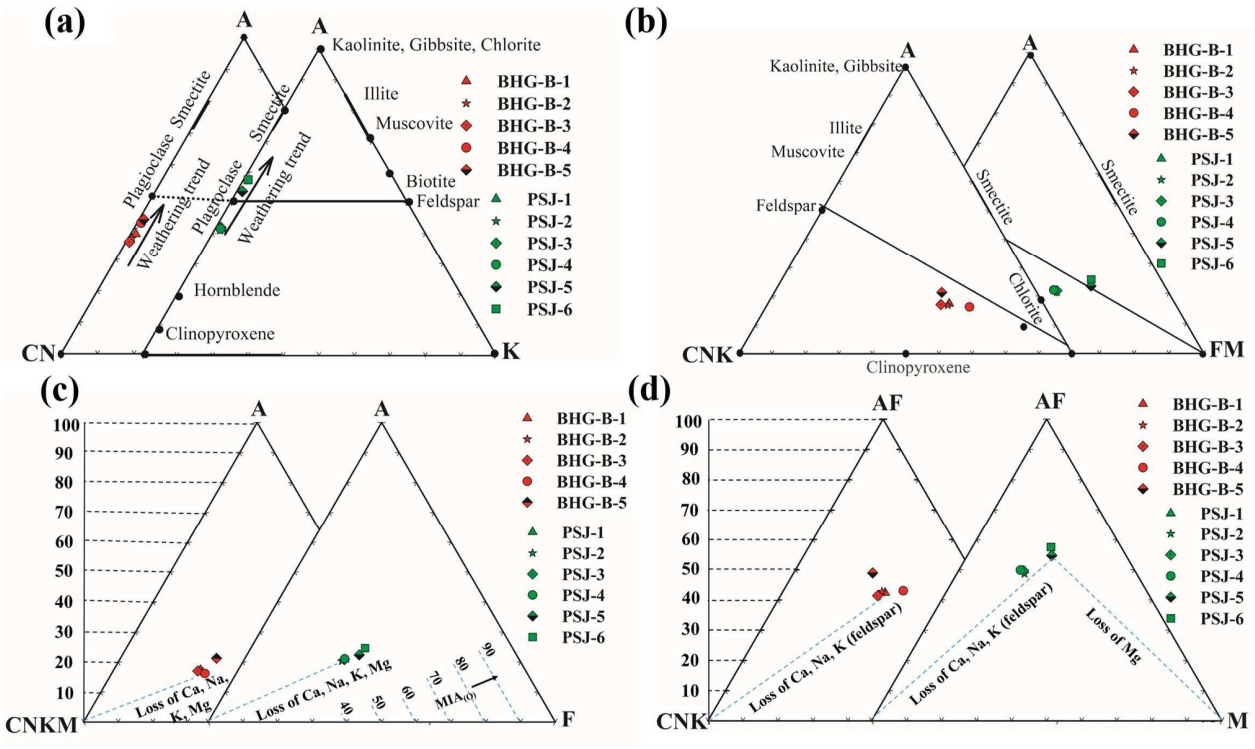

Fig. 5. (**a**) A-CN-K, (**b**) A-CNK-FM, (**c**) A-CNKM-F, and (**d**) AF-CNK-M diagrams showing weathering trends of the Bherughat and Pithampur profiles (see text for further explanations).

trends do not indicate the formation of kaolinite or gibbsite in the profile. The XRD and FTIR analyses support the presence of smectite. The plot of the sample BHG-B-5 in the A-CNK-FM, AF-CNK-M, and A-CNKM-F diagrams, suggests relative enrichment of Al and probably the formation of Al-rich smectites.The BHG-B-4 sample may have Mg-rich smectites dominantly after weathering of mafic phases. The Mg and the trace elements like Cr and Sc enrichment in the saprolite sample support smectite formation after mafic mineral weathering. Eggleton et al. (1987) and Churchman and Lowe (2012) have suggested that mafic minerals weather to trioctahedral smectites, and plagioclase weathers to dioctahedral smectite. A better understanding is required for the origin of different smectites on similar rocks and in similar conditions.

REE Geochemistry

REE provide significant insights into weathering processes. They get released from primary minerals during chemical weathering. Some are retained with the weathering products, such as clay minerals, oxyhydroxide, and phosphate phases (Jin et al., 2017). At the same time, some may get preferentially mobilized (Tripathi and Rajamani, 2007 and references therein). The mobilization could be redox controlled (e.g., Ce) or ionic size-controlled (lanthanide contraction; HREE). Such controls and variations provide essential clues to weathering of rocks.

The weathering profiles show LREE enrichment with a slight HREE depletion in the Chondrite-normalized REE plots. For Bherughat, the parent-rock and saproliths do not differ in their patterns. However, saprolite BHG-B-4 shows mobilization of REE, where HREE show more significant depletion than LREE (Fig. 6a). Eu did not mobilize after weathering of the plagioclase as Eu^{2+} oxidizes to Eu^{3+} and gets retained with clays in the saprolites (Sharma and Rajamani, 2001). Ce shows slight depletion during weathering (-ve

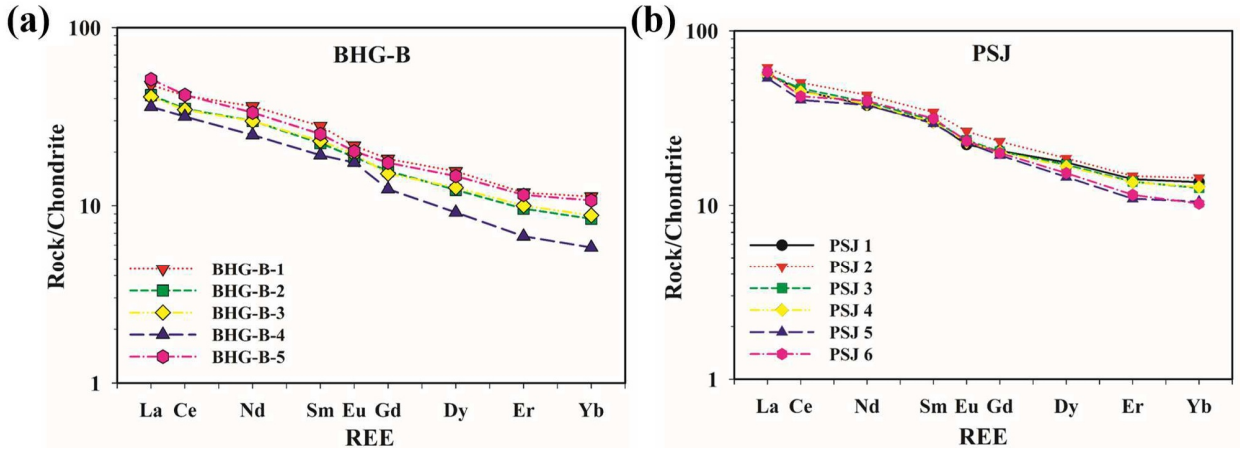

Fig. 6. Chondrite normalized REE patterns of the samples of the Bherughat (a) and Pithampur (b) weathering profiles (see text for further explanations).

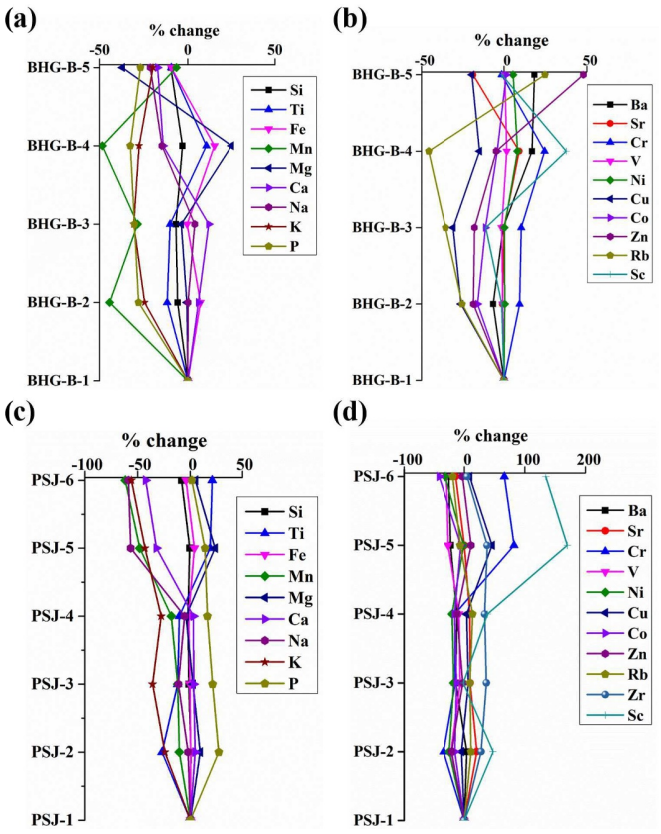

Fig. 7. The % change of major (in oxide) and trace elements of the Bherughat profile (**a** and **b**) and Pithampur profile (**c** and **d**) (see methodology for calculation). MgO enrichment along with Cr and Sc in the lower saprolites may be noted (see text for further explanations).

Ce anomalies of parent-rock: 0.95, saproliths: 0.92 and 0.93, and saprolite BHG-B-5: 0.92) (Table 1) because of mobilization as Ce^{3+}. However, saprolite BHG-B-4 (0.98) shows slight enrichment because of precipitation as Ce^{4+} oxide.

Interestingly, the chondrite normalized REE pattern of the most weathered saprolite (BHG-B-5) plots between the parent-rock and saproliths. It has been suggested that most of the REE remain concentrated in clay structures, and only minor amounts go into solution during weathering (Fleet, 1984). The saprolite BHG-B-5 horizon may have gained REE from the formerly overlying material by illuviation or leaching in the past, the overlying material has now been eroded (Tripathi and Rajamani, 2007, and references therein). Cerium's redox-controlled mobilization from the overlying horizons and its precipitation in the underlying saprolite horizon (BHG-B-5) supports this inference. The Pithampur profile shows more significant mobilization of HREE than LREE and slight Ce mobilization from the upper horizon during weathering (Fig. 6a).

From the REE geochemistry, we have observed that REE, but to a greater extent HREE, are mobile during incipient weathering of the basalts. Weathering of the primary minerals and smectite formation seem to have relatively mobilized HREE and retained LREE to give rise to a more fractionated REE pattern of the saprolites (Mongelli, 1993).

CONCLUSIONS

The following may be concluded from the mineralogical and geochemical study of the weathering profiles developed on the Deccan basalts.

1. The weathering indices and trends suggest that the basalt weathering profiles have undergone only incipient weathering. The presence of incipiently weathered profiles on the Deccan basalts, points to erosion under the neotectonic activity, which has washed away the ancient weathered material. Similarly, the perpetual exposures of the new weathering surfaces on the Deccan basalts since around 50 Ma continuously play a significant role in the consumption of CO_2 by silicate weathering.
2. Weathering of the basalts in the profiles has mainly produced smectite clays. Plagioclase rich zone may have produced Al-rich smectite. Whereas, the pyroxene rich zone may have produced Mg-rich smectite. However, a detailed clay mineral study is needed for a better understanding.
3. The REE are mobile during incipient weathering of the basalts, HREE being found more mobile. The retention of REE in the profiles is mineralogically controlled. The smectite seem to preferentialy mobilize the HREE than the LREE. The uppermost zone of the profiles shows the gain in REE due to clay illuviation or leaching of REE from the erstwhile overlying weathering zones.

Acknowledgements: AP and JKT thank DST and JNU for the financial support through the WOS-A project (SR/WOS-A/EA-51/2018) and LRE Fund. The authors thank Director, IUAC, New Delhi, for extending facilities through the MoES/P.O. (Seismic)8(090-Geochron/2012 project). The FTIR analysis by AIRF, JNU is acknowledged. Prof. Pankaj Srivastava is acknowledged for the petrographic study in his laboratory. Dr. M. M. Azam is thanked for his help during field and laboratory work.

References

Babechuk, M.G., Widdowson, M. and Kamber, B.S. (2014) Quantifying chemical weathering intensity and trace element release from two contrasting basalt profiles, Deccan Traps, India. Chem. Geol., 363, pp. 56-75.

Churchman, G.J., and Lowe, D.J. (2012) Alteration, formation, and occurrence of minerals in soils. CRC Press, pp. 1-72.

CGWB, (2013a) "District Ground Water Information Booklet", Central Groundwater Board, http://cgwb.gov.in/District_Profile/MP/indore.pdf

CGWB, (2013b) "District Ground Water Information Booklet", Central Groundwater Board, http://cgwb.gov.in/District_Profile/MP/Dhar.pdf

Conwell, C.T., Saltzman, M.R., Edwards, C.T., Griffith, E.M. and Adiatma, Y. D. (2022). Nd isotopic evidence for enhanced mafic weathering leading to Ordovician cooling. Geology. doi: 10.1130/G49860.1

Eggleton, R.A., Foudoulis, C. and Varkevisser, D. (1987) Weathering of basalt: changes in rock chemistry and mineralogy. Clays and Clay Minerals, v.35(3), pp.161-169.

Fedo, C.M., Wayne Nesbitt, H. and Young, G.M. (1995) Unravelling the effects of potassium metasomatism in sedimentary rocks and palaeosols, with implications for paleo weathering conditions and provenance. Geology, v.23(10), pp.921-924.

Fleet, A. J. (1984) Aqueous and sedimentary geochemistry of the rare earth elements. *In:* Developments in Geochemistry, Elsevier, 2, pp.343-373.

Griffin, G.M. (1971) Interpretation of X-ray diffractogram data. *In:* R.E. Carver (Ed.), procedures in sedimentary petrology, Wiley, New York, pp.541-569.

Goddéris, Y., Donnadieu, Y., Tombozafy, M. and Dessert, C. (2008) Shield effect on continental weathering: implication for climatic evolution of the Earth at the geological timescale. Geoderma, v.145(3-4), pp.439-448.

Heiri, O., Lotter, and A. F., Lemcke, G. (2001) Loss on ignition as a method for estimating organic and carbonate content in sediments: reproducibility and comparability of results. Jour. Paleolimnology, v.25(1), pp.101-110.

Jiang, K., Qi, H.W., Hu, R.Z. (2018) Element mobilization and redistribution under extreme tropical weathering of basalts from the Hainan Island, South China. Jour. Asian Earth Sci., v.158, pp.80-102.

Kent, D. V. and Muttoni, G. (2013) Modulation of Late Cretaceous and Cenozoic climate by variable drawdown of atmospheric pCO_2 from weathering of basaltic provinces on continents drifting through the equatorial humid belt. Climate of the Past, v.9(2), pp.525-546.

Khanna, P.P., Saini, N.K., Mukherjee, P.K. and Purohit, K.K. (2009). An appraisal of ICP-MS technique for determination of REEs: long term QC

assessment of silicate rock analysis. Himal. Geol., v.30 (1), pp.95–99.

Kaotekwar, A.B., Meshram, R.R., Sathyanarayanan, M., Krishna, A.K. and Charan, S.N. (2014). Structures, petrography and geochemistry of Deccan basalts at Anantagiri hills, Andhra Pradesh. Jour. Geol. Soc. India, v.84(6), pp. 675-685.

Klein, C. and Philpotts, A. (2013) Earth Materials: Introduction to Mineralogy and Petrology. Cambridge University Press, 577p.

Kumpulainen, S., and Kiviranta, L. (2010) Mineralogical and chemical characterization of various bentonite and smectite-rich clay materials Part A: Comparison and development of mineralogical characterization methods Part B: Mineralogical and chemical characterization of clay materials (No. POSIVA-WR—10-52). Posiva Oy.

Ling, S., Wu, X., Zhao, S. and Liao, X. (2018) Evolution of porosity and clay mineralogy associated with chemical weathering of black shale: a case study of Lower Cambrian black shale in Chongqing, China. Jour. Geochem. Explor., v.188, pp. 326-339.

Liu, X., Mao, X., Yuan, Y. and Ma, M. (2019) Aeolian accumulation: an alternative origin of laterite on the Deccan Plateau, India. Palaeogeo., Palaeoclimat., Palaeoeco., v.518, pp. 34-44.

Jin, L., Ma, L., Dere, A., White, T., Mathur, R. and Brantley, S.L. (2017) REE mobility and fractionation during shale weathering along a climate gradient. Chem. Geol., v.466, pp. 352-379.

Masuda, A., Nakamura, N. and Tanaka, T. (1973) Fine structures of mutually normalized rare-earth patterns of chondrites. Geochim. Cosmochim. Acta, v.37(2), pp.239-248.

Mongelli, G. (1993) REE and other trace elements in a granitic weathering profile from “Serre”, southern Italy. Chem. Geol., v.103(1-4), pp.17-25.

Nesbitt, H.W. and Markovics, G. (1997) Weathering of granodioritic crust, long-term storage of elements in weathering profiles, and petrogenesis of siliciclastic sediments. Geochim. Cosmochim. Acta, v.61(8), pp.1653-1670.

Nesbitt, H.W. and Young, G.M. (1989) Formation and diagenesis of weathering profiles. Jour. Geol., v.97(2), pp.129-147.

Parmar, S., and Sharma, S. K. (2020). Estimation of Soil Loss and Soil Erodibility for Different Crops, Nutrient Managements and Soil Series. Indian Jour. Pure App. Biosci., v.8(1), pp.204-212.

Peshwa, V.V., and Kale, V.S. (1997) Neotectonics of the Deccan Trap Province: Focus on the Kurduwadi Lineament: Jour. Geophys., v.18(1), pp.77–86.

Raj, R., Tripathi, J. K., Kumar, P., Singh, S. K., Phartiyal, B., Sharma, A., Sridhar, A., Chamyal, L. S. (2021) Palaeoclimatic and sea-level fluctuations from the last deglaciation to late Holocene from western India: Evidence from multiproxy studies, Jour. Asian Earth Sci., v.214, doi:10.1016/j.jseaes.2021.104777.

Rau, G. H., Knauss, K. G., Langer, W. H. and Caldeira, K. (2007) Reducing energy-related CO_2 emissions using accelerated weathering of limestone. Energy, v.32(8), pp.1471-1477.

Reddy, S. J. (1983) Agroclimatic classification of the semiarid tropics I. A method for the computation of classificatory variables. Agricultural Meteorology, v.30(3), pp.185-200.

Roy, S. (2006) Sedimentary manganese metallogenesis in response to the evolution of the Earth system. Earth Sci. Rev., v.77(4), pp.273-305.

Sharma, A., and Rajamani, V. (2001) Weathering of charnockites and sediment production in the catchment area of the Cauvery River, southern India. Sediment. Geol., v.143(1-2), pp.169-184.

Srivastava, P., Siddaiah, N.S., Sangode, S.J. and Meshram, D.C. (2018) Mineralogy and geochemistry of various colored boles from the Deccan volcanic province: implications for paleoweathering and paleoenvironmental conditions. Catena, v.167, pp.44-59.

Taylor, S.R. and McLennan, S.M. (1985) The continental crust: its composition and evolution. Blackwell Scientific Publications, Oxford, 312p.

Tripathi, J.K. and Rajamani, V. (2007) Geochemistry and origin of ferruginous nodules in weathered granodioritic gneisses, Mysore Plateau, Southern India. Geochim. Cosmochim. Acta, v.71(7), pp.1674-1688.

Tripathi, J.K., Bock, B. and Rajamani, V. (2013) Nd and Sr isotope characteristics of Quaternary Indo-Gangetic plain sediments: Source distinctiveness in different geographic regions and its geological significance. Chem. Geol., 344, pp.12-22.

Vaidyanadhan, R. and Ramakrishnan, M. (2008) Geology of India (vol. 1 & 2). Geological Society of India, Bangalore, 994p.